applied sciences

MDPI

Article

An Experimental Study on the Dynamic Behavior of an Ultra High-Strength Concrete

Ahmet Reha Gunay [1], Sami Karadeniz [2,*] and Mustafa Kaya [3]

[1] TUBITAK-SAGE Defense Industries Research and Development Institute, Ankara 06261, Turkey; reha.gunay@tubitak.gov.tr
[2] Mechanical Engineering Department, Baskent University, Ankara 06790, Turkey
[3] Aerospace Engineering Department, Ankara Yildirim Beyazit University, Ankara 06050, Turkey; mukaya@ybu.edu.tr
* Correspondence: skaradeniz@baskent.edu.tr; Tel.: +90-532-350-1882

Received: 15 May 2020; Accepted: 15 June 2020; Published: 17 June 2020

Featured Application: In recent years, a fast progress has been observed in the development of ultra-high-strength concrete (UHSC). This type of concrete is designed to achieve size efficiency in many structural members, especially those subjected to the impact and blast types of loading conditions. Numerical simulation of structures made of UHSC mixtures under such loading conditions requires an experimentally obtained stress–strain response for different strain rates so that this information may be fed into computer codes.

Abstract: Ultra-high-strength concrete is a newly developed construction material that has a minimum 120 MPa or higher compressive strength. Recently, the usage of high-strength and ultra-high-strength concretes has become widespread due to the enhancement of the concrete technology. Many civil engineering structures constructed by using concrete materials are usually subjected to, in addition to static loads, dynamic loads due to earthquakes, wind and storm, impact and blast, which take place under high energy and high strain rate values. The effects of such loadings on the structure must be understood thoroughly. In recent years, the withstanding of a structure on these loading conditions has become a crucial issue for its impact on the economy and human safety. One of the approaches to fulfill these requirements is to develop high-strength or ultra high-strength concretes (UHSCs). In this study, an ultra-high-strength concrete with a compressive strength of 135 MPa was designed and developed. In order to determine the dynamic behavior of this UHSC, the specimens at three height/diameter ratios (approximately, 0.6, 1.0 and 1.2) were extracted from the prepared concrete mixtures. These concrete specimens were tested to determine both the quasi-static and dynamic compressive behaviors of the developed concrete. In the quasi-static compression tests, cylindrical specimens and a conventional compressive testing machine were used. In order to study the dynamic compressive behavior, a Split Hopkinson Pressure Bar (SHPB) test setup was used. In this test system, the time variations of compressive strength, the strain and strain rates under uniaxial pressure loading were experimentally evaluated and the deformation and fracturing processes of the specimens were recorded using a high-speed camera. The test results, based on the testing of 21 different specimens, have shown that the dynamic compressive strength values of the developed concrete varied in the range of 143 to 253 MPa, while the strain rate values varied in the range of 353 s^{-1} to 1288 s^{-1}. Using the data generated in the SHPB tests, the parameters present in a Johnson–Holmquist–Cook concrete material model, which is used in numerical studies on the high strain rate behavior of concretes, were evaluated.

Keywords: ultra high-strength concrete; dynamic behavior; high strain rate; Split Hopkinson Pressure Bar; Johnson–Holmquist–Cook concrete model

1. Introduction

Normal strength concretes are produced by mixing mainly cement, aggregate and water. They are the most widely used construction material in buildings, dams, port structures, bridges, tunnels and skeletons of factory buildings, etc. The development of concrete technology has always been a continuing process, both in the past and in the present day. Today, there are more than 25 types of concrete in use in the construction industry. One of the areas of current development in concrete or concrete structures focuses mainly on the improvements in strength, durability and workability of various concrete mixtures. However, instead of normal-strength concretes, high-strength and ultra-high-strength concretes are being developed to meet the requirements of the some special construction works. The use of high-strength concrete in both the classical concrete sector and in the concrete prefabrication sector has increased, especially during the 1980s [1,2]. Since then, the specially designed and produced concretes became the preferred material used in the construction of special purpose strategic buildings, such as nuclear plants, hangars and operation control centers.

There is no universally accepted classification of the concrete types. Nevertheless, the concretes possessing a range of 60 to 125 MPa compressive strength are regarded as high-strength concretes (HSC), while concretes having a compressive strength higher than 125–140 MPa are termed as ultra-high-strength concretes (UHSCs). Apart from their superior compressive strength properties, these types of concretes should also possess some generally desired properties such as high workability, low shrinkage, self-compaction and discharge properties. The ultra-high-strength concretes are produced by mixing good quality cement and aggregate with super plasticizer and silica fume as the main constituent materials, and decreasing the water/cement ratio up to the order of 0.20 [3].

Generally, the first step in the concrete development studies both on the normal and high-strength or ultra-high-strength concretes is to obtain information on the experimental behavior of the concrete under the quasi-static loading conditions at a strain rate of approximately 10^{-5} to 10^{-6} s^{-1}. However, in the present day, the concrete structures are exposed to not only loadings that can be considered as quasi-static loadings in nature, but also to extreme dynamic loading conditions due to natural disasters (storm, flood, earthquake, etc.) and dynamic factors like high-energy impact and blast. These types of dynamic loads may cause permanent failures and damage to the material. The research studies on the behavior of concrete structures subjected to extreme loading conditions show that a better understanding of the response of high-strength or ultra high-strength concretes may open the way to novel applications of these types of concrete [4,5]. Therefore, for a complete development of a modern mixture of a concrete material, the behavior under both the quasi-static and dynamic loading conditions and the strain rate effects must be also considered. Figure 1 shows the approximate ranges of the expected strain rates for some common loading situations and the applicable testing techniques.

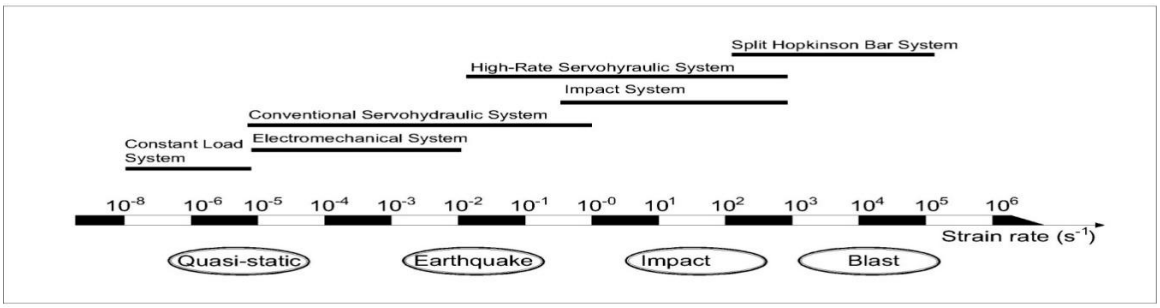

Figure 1. Strain rates associated with different types of loading and applicable test techniques.

Although it is well known that many concrete structures have to withstand dynamic loading conditions, the studies on the dynamic behavior of concrete are very limited compared with the available data in the literature on the static or the quasi-static loading responses. In addition, there is a limited number of numerical and experimental studies reported on the behavior of concretes under

high strain rate conditions. Bischoff and Perry [6], in their study on the behavior of concrete under high strain rates, presented the test methods used and the strain rates that were achieved in the previous studies. Bresler and Bertero [7] and, Takeda and Tachikawa [8], obtained testing data for strain rates above 1 s^{-1} by using hydraulic testing machines. Hughes and Gregory [9], Watstein [10], and Hughes and Watson [11] achieved strain rate levels on the order of 10 s^{-1} using a drop-weight impactor.

Especially, in last two decades, it has become possible to observe the dynamic compressive behavior of the concretes under strain rates of 10^2–10^3 s^{-1} using the Split Hopkinson Pressure Bar (SHPB) test setups. Additionally, in some high strain rate studies on fiber-reinforced normal and high-strength concrete samples that had compressive strength values of 35–110 MPa, strain rates in the range of 10 to -700 s^{-1} were measured by using SHPB test setups [12–17]. In these experimental studies, the specimens having radii varying in the range of 50 to 75 mm, and a length of 37.5 mm, were used. It is well known that it is almost impossible to produce concrete specimens that have uniform composition due to difficulties involved in controlling the mixture content of a concrete. On the other hand, there exists a small number of experimental studies in which specimens with a radii in the range of 10 to 15 mm were used [18,19]. In these works, the attained strain rates were relatively high, varying in the range of 700–1700 s^{-1}. Nowadays, to improve, especially, the tensile properties of concretes, different types of fibers have been used in the UHSC productions [20,21]. Using reinforced concrete specimens with the fiber volume ratios of 0.5%, 1%, and 1.5%, the energy dissipation, the crack initiation capacities and the dynamic behavior under the high strain rates were studied both experimentally by using SHPB setups and numerically [22–25]. By using the SHPB test results, a number of numerical verification studies was also reported in the literature [26–28].

In recent years, studies on the dynamic behavior of concrete materials has intensified on Reactive Powder Concretes (RPC), which show high strength, durability and fracture properties. The static and dynamic strengths, the dynamic increase factor (DIF), the effects of strain rate and the effects of the geometric size of the specimens were discussed in a recent review paper [29].

In the available literature, there exist some deficiencies in the discussion of the data that may be extracted from the SHPB tests so that they can be transferred into the numerical data base required in numerical modeling of concrete materials subjected to extreme loading conditions. So, there is a need to extend the data, especially on the parameters generated by making use of the SHPB data. Therefore, using such numerical data, fed into available computer codes, may ease both the experimental and numerical studies of the behaviors of structures made of high or ultra high-strength concretes. The RPC is the most popular ultra strength type of concrete but RPC requires special production methods: its cost of construction is relatively higher than that of constructions based on conventional methods. For this reason, the concrete which is conventionally (low water/cement ratio, use of GGBF slag to fill the gaps) produced in this work was preferred in spite of the fact that its workability is low.

In this study, an ultra-high-strength concrete with a compressive strength of 135 MPa has been designed and produced. To determine the behavior of the high-strength concrete under dynamic loading conditions, specimens of different sizes were produced by using a water jet cutting machine. These specimens were cut from the same concrete test samples that were prepared for the quasi-static tests. The SHPB data were utilized to determine the parameters of the Johnson–Holmquist–Cook material model by using an in-house developed computer code on the MATLAB environment. The Johnson–Holmquist–Cook model is one of the material models available in most computational software, such as LS-DYNA.

As mentioned above, there exists a need for available data on the dynamic behavior of UHSC materials. The UHSC is known to have same advantages in terms of ballistic penetration (which takes place at strain rates in the range of 10^2–10^3 s^{-1}) performance when compared to conventional concrete, since it has higher strength. However, UHSC has disadvantages such as its brittle structure, which is less deformable. This work mainly focuses on the evaluation of the effects of the SHPB test conditions on the behavior of the developed ultra high-strength concrete. Hence, the main emphasis of the present study is to contribute to a better understanding of the subject. For this purpose, it has been considered

that the results obtained will provide important data for future works involving numerical studies and the interpretation of test results on the ultra high-strength concrete structural members under impact and blast loading conditions.

2. Development of Ultra High-Strength Concrete

In the constituents of the mixture of the developed ultra high-strength concrete, sand of 0–5 mm, fine aggregate of 5–12 mm, coarse aggregate obtained from limestone of 12–19 mm and 19–25 mm, Portland cement, ground granulated blast furnace slag (GGBF slag) and super plasticizer were used. During the production process, the concrete became workable after adding water and super plasticizer to the mixture of cement, GGBF slag and aggregates, which are manufactured in dry form and blended for a time period of 3–4 min in the mixer. The composition of the developed concrete mixture is shown in Table 1.

Table 1. Composition of the ultra-high-strength concrete.

Materials	Quantity (kg/m^3)	Ratio (%) (Volume)
Cement	450	
GGBF slag	45	
Sand (0–5 mm)	39	
Limestone (5–12 mm)	33	
Limestone (12–19 mm)	16	
Limestone (19–25 mm)	12	
Water/Cement		13
Super Plasticizer		2.5

The workability of the concrete obtained in the concrete mixer was very low. The measured slump values were observed to be between 0–1. Therefore, the mixture was placed within cylindrical sample containers having dimensions of Ø150 × 300 mm with the help of 3-stage ramming on the vibrating plate, in order to avoid segregation and to obtain a compact and homogeneous structure. The hardened concrete samples have been cured in a cure room at a temperature of 24 °C and a humidity of 97% until the quasi-static tests. The quasi-static tests were carried out at a strain rate of 10^{-5} s^{-1} in a compression test device, as shown in Figure 2a. A photo of the specimen used in these compression tests is shown in Figure 2b.

(**a**) (**b**)

Figure 2. (**a**) Quasi-static test setup. (**b**) A cylindrical specimen after testing.

In order to observe the results of the strengthening process, the samples were tested for failure on the 1st, 7th, 28th and 56th days following production. Three samples were tested on each test day. The average strength of the three samples was calculated for the compressive strength values of the daily testing samples. The variation of the quasi-static compression test results are given in Table 2.

Table 2. Compressive strength values of the ultra high-strength concrete.

Item Number	Day after Production	Average Strength (MPa)	Standard Deviation
1	1	108	7.35
2	7	115	7.84
3	28	125	3.70
4	56	135	3.22

3. Experimental Work

3.1. Sample Preparation for the Dynamic Tests

The sample preparation process started after completing the quasi-static tests following the development of the ultra high-strength concrete. Initially, the specimen production was planned for three different specimen samples with a diameter of D = 10 mm with lengths of L = 6, 10 and 12 mm. The test specimens were produced from the same cylindrical sample batch (Ø150 × 300 mm) that was used in the quasi-static tests by using a water jet cutting machine. The water jet cutting method is used for enabling to cut geometries in a high precision by transferring the high-pressure water to the cutting machine through pumps of a high flow rate. In the first stage, a number of circular disks at thicknesses of 6, 10 and 12 mm were cut from the Ø150 × 300 mm sample blocks. In the second stage, the circular disks were cut with a diameter of 10 mm. Two photos of the water jet cutting process are shown in Figure 3.

(**a**) (**b**)

Figure 3. Water jet cutting: (**a**) Cutting of circular disks at thicknesses of 6, 10 and 12 mm. (**b**) Cutting of a circular disk at a diameter of 10 mm.

Following the cutting process, surface smoothing was carried out using a sanding machine. At the end, test specimens with approximate length/diameter ratios of L/D = 0.6, 1.0 and 1.2 were produced. Photographs of these three different specimens are shown in Figure 4.

(**a**) (**b**) (**c**)

Figure 4. Approximate length to diameter ratios of the test specimens: (**a**) L/D = 1.20; (**b**) L/D = 1.00; (**c**) L/D = 0.60.

3.2. Split Hopkinson Pressure Bar Tests and Discussion

The dynamic behavior tests for the developed ultra-high-strength concrete were carried out in a Split Hopkinson Pressure Bar (SHPB) test unit. This setup is a commonly used experimental device to determine the behavior of materials under high strain rate loadings. The SHPB test systems were first invented by Hopkinson [30] to determine the dynamical characteristics of the materials, and then improved by Kolsky [31]. One of the detailed works on the applications of SHPB systems in concrete studies was given by Ross and Tedesco [32]. The SHPB test unit used in the present study essentially consisted of a gas tank, striker bar, incident bar, transmitter bar and an absorber system together with a section where the specimen is placed. Moreover, a pulse shaper to decrease the effects of other frequencies, a momentum trap to provide the linear transfer of the elastic wave amplitude from the striker to the incident bar, and strain gauges to measure the strain values, were used. The sample ends were lubricated with vacuum grease. A schematic illustration of the test setup is shown in Figure 5.

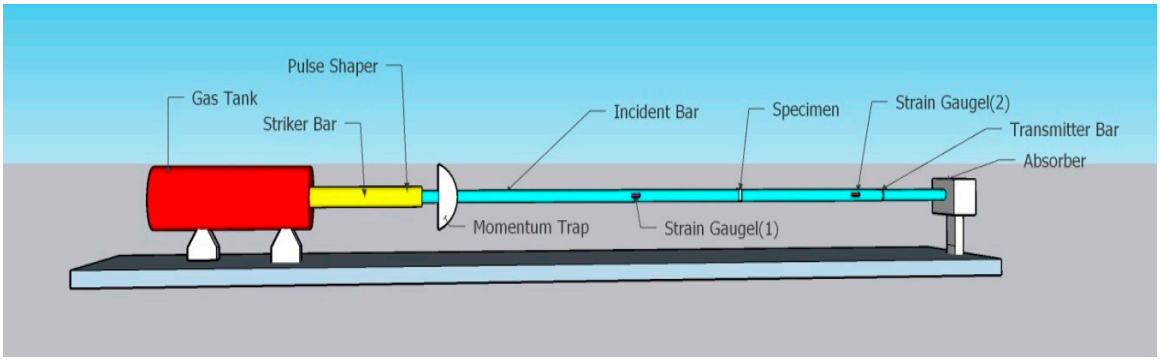

Figure 5. Schematic drawing of the Split Hopkinson Pressure Bar (SHPB) test setup.

A photo of a sample placed between the incident and transmitter bars is shown in Figure 6.

The working principle of a split Hopkinson pressure bar test device is based upon the wave propagation in materials. In a split Hopkinson bar test, the impact of the striker bar on the loading block side induces a longitudinal compressive wave. After the wave arrives at the incident bar–specimen interface, a part of this wave is reflected as ε_r, while the other part of the wave, denoted as ε_t, continues to propagate through the specimen and into the transmitted bar. The stress wave pulses on the incident and transmitted bars are recorded by a Wheatstone bridge, formed by the strain gauges mounted on the incident and transmitted bars. In this test rig, all of the bars are made of maraging steel and have a diameter of 19 mm. The striker bar is 300 mm long while each of the incident and transmitter bars is 3340 mm long.

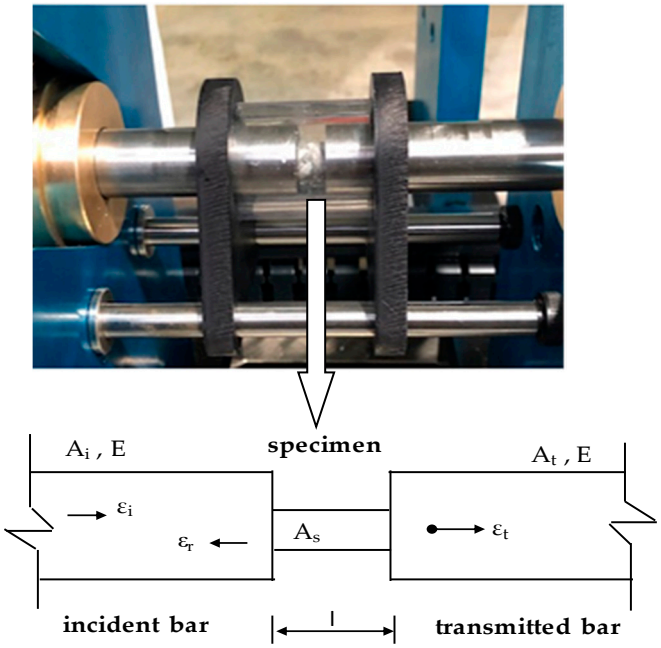

Figure 6. The incident and transmitter bars and the specimen in the SHPB test setup.

The data acquired as the time-varying voltage measurement during the experiment was evaluated to calculate the stress, the strain rate and the strain values by using Equations (1)–(3), respectively. The calculations were carried out at intervals according to the time duration observed on the time–voltage plot. An example of the time variation of the measured voltage data is given in Figure 7. It should be noted that the waves produced by the momentum trap were not considered in the calculations.

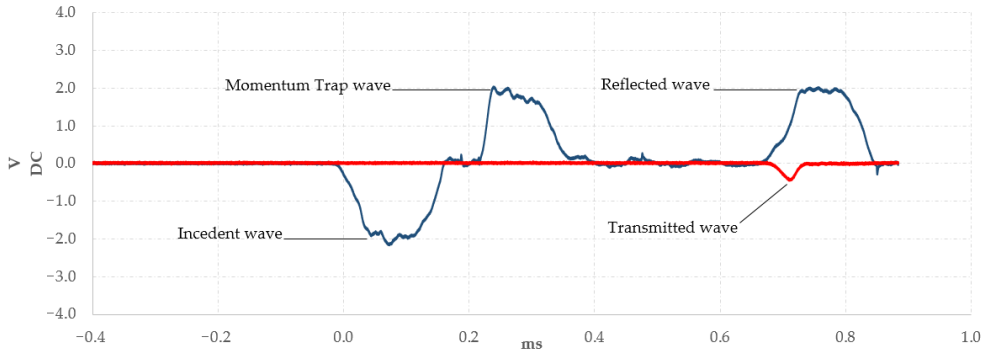

Figure 7. A sample of measured time variation of voltage during the SHPB test.

$$\sigma(t) = E_b \frac{A_b}{As}\, \varepsilon_t(t) \tag{1}$$

$$\dot{\varepsilon}(t) = \frac{-2c_b}{l}\varepsilon_r(t) \tag{2}$$

$$\varepsilon(t) = \frac{-2c_b}{l}\int_0^t \varepsilon_r(\tau)d\tau \tag{3}$$

Equations (1)–(3) are well explained in the literature regarding the Split Hopkinson Pressure Bar tests [33,34]. In these equations, ε_t represents the transmitted wave, whilst ε_r represents the reflected wave. E_b, A_b and c_b represent the modulus of elasticity, cross-sectional area and the elastic wave velocity, respectively. A_s and ℓ indicate the cross-sectional area and the length of the specimen, respectively.

The time variations of the stress and the strain for the ultra-high-strength concrete were calculated by evaluating the time-voltage data are shown in Figure 8. Using the data extracted from Figure 8c, the average strain rate for this test has been evaluated as 720.3 s^{-1}.

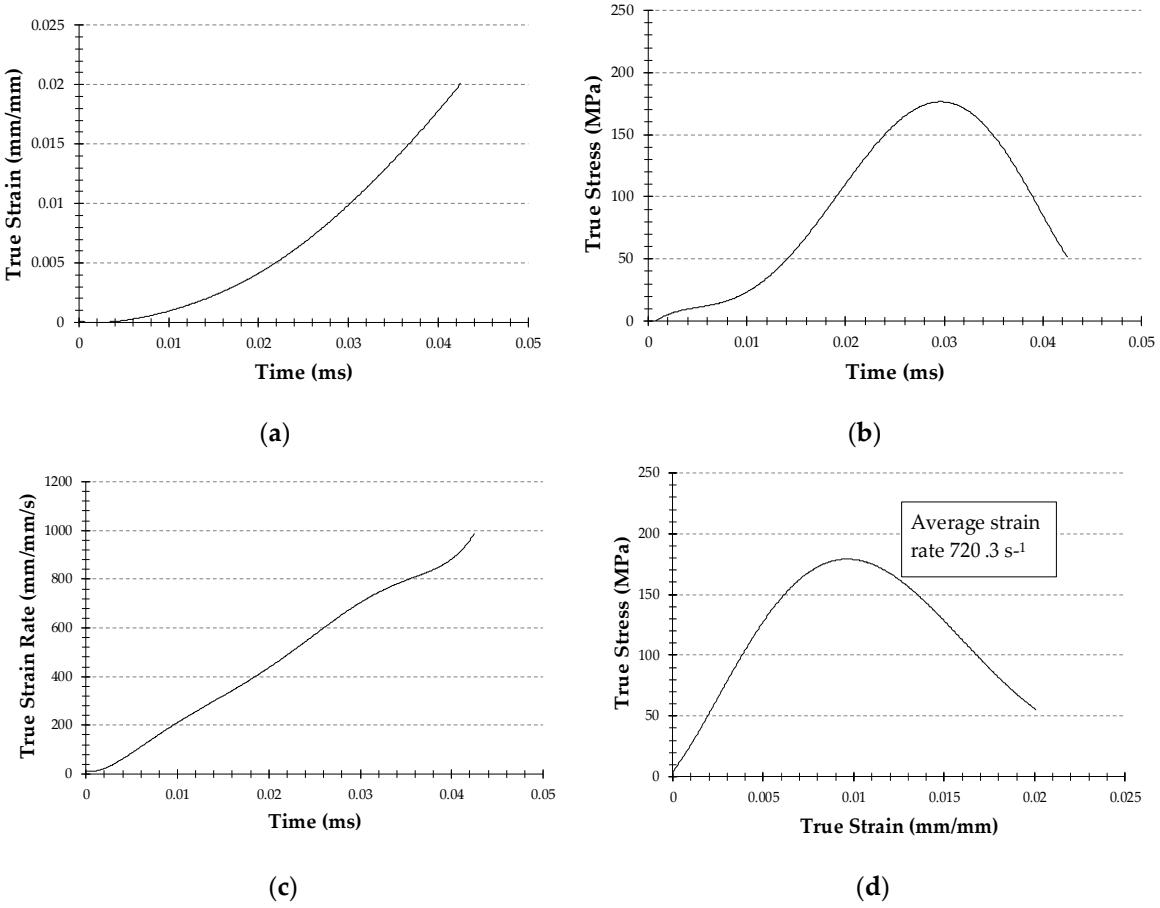

Figure 8. UHSC-16 (Ultra High Strength Concrete—Specimen number 16) SHPB test results: (**a**) true strain-time; (**b**) true stress-time; (**c**) true strain rate-time; (**d**) true stress–strain relations.

The SPHB test system available does not allow much higher sample sizes. This is one of the reasons for using 10 mm diameter samples, although some aggregate sizes are greater than 20 mm. The samples used were obtained by water jet cutting. Therefore, the strength conditions at cutting edges may differ. In order to eliminate these differences, 28 tests were performed. However, results from 21 tests were used since the other 7 tests appeared not to reflect the expected homogeneous behavior of the concrete. As stated above, in the tests, three groups of specimens were used. The test pressure was selected from the range of 0.1 to 0.3 MPa, while the striker speed was in the range of 7.89–13.48 m/s. The test results of 21 specimens are given in Table 3. In these tests, the standard deviations concerning the strength, strain and strain rate values are 30.34 MPa, 0.009 and 262.68 s^{-1}, respectively.

A high-speed camera was also used in this study to visualize the dynamic behavior of the ultra-high-strength concrete. The high-speed camera recorded the test process at a frame rate of the microsecond order. Figure 9a shows the instantaneous states of a sample at 6 different time instances, while the corresponding stress–strain relation is given in Figure 9b. The numbered labels in Figure 9b correspond to the 6 frames given in Figure 9a.

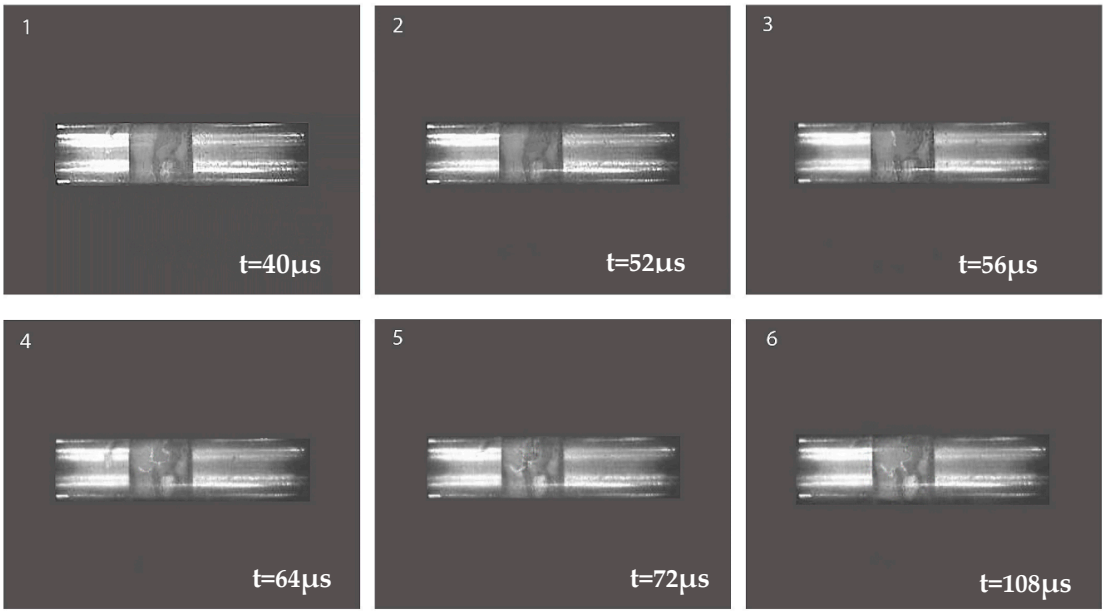

(**a**)

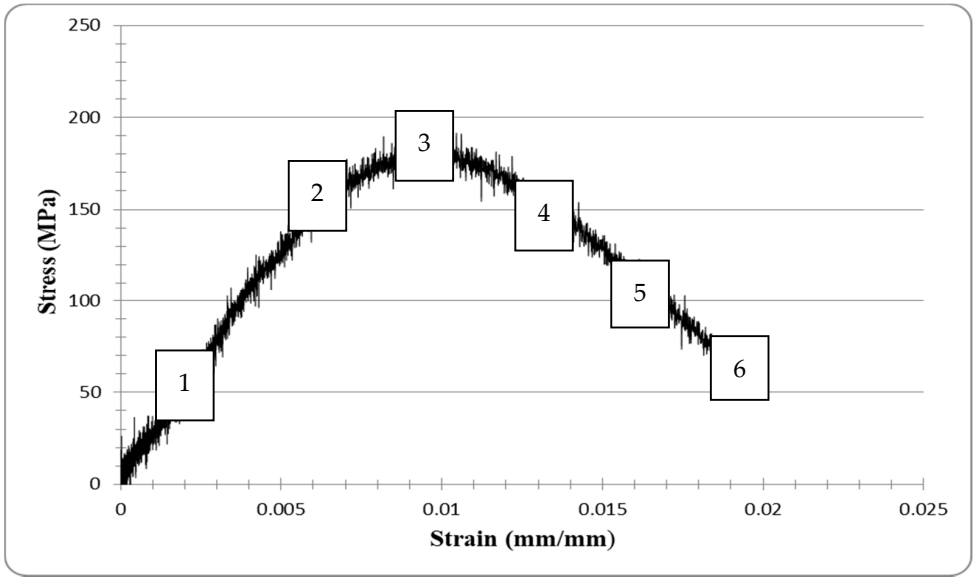

(**b**)

Figure 9. The true stress–true strain behavior of specimen UHSC-16 during the maximum strain rate of about 960 s^{-1}: (**a**) High-speed test visualization of the sample UHSC-16; (**b**) Stress–strain relation for the specimen UHSC-16.

In the first frame, the sample seems to behave elastically. The stress–strain curve is also linear in the period of 0 to 40 μs. During this stage, the strains are reversible. The first failure behavior, the first fracture, is observed in the second frame. The specimen is now possessing a non-linear stress–strain relation, which means that after this point the strains are irreversible. In the third frame, the spreading of cracks and the deeper fractures are observed to occur in the regions close to the location with the first failure. It has been considered that at this stage the specimen well exceeds its compressive strength since the local failures are spread out. The spreading of the fractured regions due to decrease in stress level are observed in the fourth frame. In the last two frames, the stress level decreases, cracks and fractures are now everywhere. Finally, the dynamic load carrying capacity of the ultra-high-strength concrete specimen reaches its lowest point after breaking away of the pieces from the specimen.

Table 3. Compressive strength values of the ultra-high-strength concrete.

Specimen No	Length/ Diameter Ratio	Pressure of Test (MPa)	Impact Velocity (m/s)	Dynamic Peak Stress (MPa)	Dynamic Strain at Peak Stress	Peak Strain Rate 1/s	DIF (Dynamic Increase Factor) for Peak Stress
UHSC-1	0.56	0.12	8.46	146	0.027	1109	1.08
UHSC-2	0.56	0.15	7.92	162	0.02	963	1.20
UHSC-3	0.57	0.12	8.53	143	0.048	1288	1.06
UHSC-4	0.57	0.15	11.12	231	0.01	549	1.71
UHSC-5	0.80	0.27	12.64	253	0.012	753	1.87
UHSC-6	0.81	0.30	13.48	210	0.007	593	1.56
UHSC-7	0.81	0.20	11.10	150	0.017	1257	1.11
UHSC-8	0.82	0.23	11.86	223	0.009	545	1.65
UHSC-9	0.82	0.20	11.14	163	0.011	584	1.21
UHSC-10	0.82	0.17	9.99	209	0.011	531	1.55
UHSC-11	0.82	0.30	13.38	180	0.015	950	1.33
UHSC-12	0.83	0.20	10.97	195	0.009	523	1.44
UHSC-13	1.06	0.20	11.04	154	0.027	814	1.14
UHSC-14	1.08	0.27	12.68	158	0.019	843	1.17
UHSC-15	1.08	0.10	7.84	198	0.027	602	1.33
UHSC-16	1.09	0.30	13.35	191	0.02	960	1.41
UHSC-17	1.10	0.23	11.77	166	0.013	696	1.23
UHSC-18	1.15	0.30	13.45	166	0.017	835	1.23
UHSC-19	1.16	0.20	10.94	170	0.008	461	1.26
UHSC-20	1.17	0.20	11.12	163	0.012	515	1.21
UHSC-21	1.18	0.10	7.89	164	0.011	353	1.21

In the dynamic compression tests, the length to diameter ratio ranging from 0.5 to l.0 is acceptable. In order to diversify the strain rates and to see the size effects, the specimens having the length/diameter ratios varying in the range of 0.56 to 1.18 were used. As it is seen in Figure 10, As it is seen in this figure, under the same test conditions, the strain rates measured in specimens with lower length/diameter ratios are higher than those obtained for the specimens having a relatively higher ratios. This was an expected result for a specimen cut from a homogenous and linear isotropic material. Although, the concrete specimens used in these tests were not made of a homogeneous material, the strain rate are calculated from Equation (4) as

$$\dot{\varepsilon} = \frac{v_2 - v_1}{\ell} \tag{4}$$

where v_1 and v_2 are the output and input velocities, respectively, and ℓ is the length of the specimen.

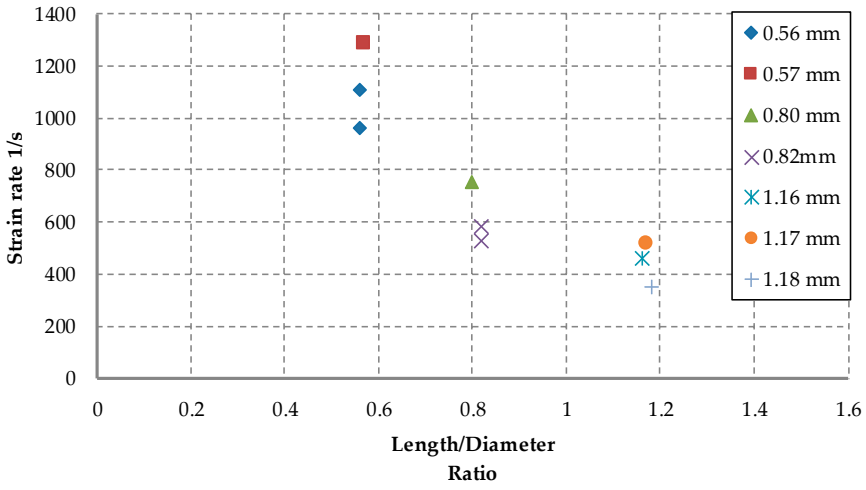

Figure 10. Strain rate and length/diameter ratio relations.

In order to observe the effects of test pressure on the dynamic response the test pressure was varied in the range of 0.1 to 0.3 MPa. The variation of the strain rate with the test pressure is shown in Figure 11. As it is seen in the Figure 11, the strain rate increases almost linearly as the test pressure increases.

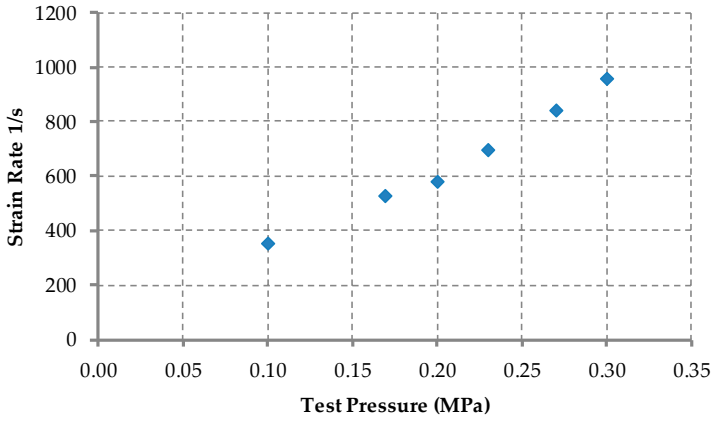

Figure 11. Strain rate and test pressure relations.

The measured dynamic compressive strength values are given in the fifth column in Table 3. As expected, the peak stress values show some variations due to the brittle nature of the concrete and the variations of the constituent ratios in each specimen. Nevertheless, the peak values remained within a range of 143 to 253 MPa. The last column in Table 3 contains the percentage increase in the strength of the UHSC with respect to the maximum quasi-static strength of 135 MPa.

3.3. Material Characterization Based on the SPHB Data

A total of 21 samples of ultra high-strength concrete were tested in the Split Hopkinson Bar (SPHB) test system and the primary measured values are given in Table 3. The tests also provided time variations of the stress, strain and strain rate values. Strain rates in the range of 353–1288 s^{-1}, which are typical values under impact and blast effects, were observed during the tests.

The Johnson–Holmquist–Cook (JHC) model is one of the material models developed to numerically analyze the concrete behavior under impact and blast effects. It is a kind of elastic-viscoplastic model proposed by Holmquist [35]. The model is known to handle the high strain, high strain rate and high pressure cases in concretes. The commercial hydrocode LS-DYNA included the JHC model as a material model in 1997 [36]. The JHC material model consists of the relations for strength, damage and equation of state.

3.3.1. Strength

The main equation of the JHC material model is given as follows:

$$\sigma^* = [A(1 - D) + BP^{*N}](1 + C\ln\dot{\varepsilon}^*) \quad (5)$$

where $\sigma^* = \sigma/f_c$ and $P^* = P/f_c$ are normalized stress and pressure, respectively. σ is the equivalent stress, P is the pressure and f_c is the characteristic pressure strength. $\dot{\varepsilon}^* = \varepsilon^*/\varepsilon^*_0$ is the normalized strain rate, where ε^* and ε^*_0 are the strain rate and reference strain rate, respectively. A, B, C and N are the model parameters to be determined.

3.3.2. Damage

The JHC material model also has a damage expression to model the failure, as given below:

$$D = \sum \frac{\Delta\varepsilon_P + \Delta\varepsilon\mu_P}{\varepsilon^f_P + \mu^f_P} \quad (6)$$

where $\Delta\varepsilon_P$ is the effective plastic strain change and $\Delta\varepsilon\mu_P$ is the plastic volume change under constant pressure. $\varepsilon_P^f + \mu_p^f$ is the total plastic strain under constant pressure until the failure happens according to the following relation:

$$\varepsilon_P^f + \mu_p^f = D_1 \left(P^* + T^*\right)^{D_2} \geq E_{fmin} \quad (7)$$

where $T^* = T/f_c$ is the normalized tension stress, and where T is the tension stress. D_1 ve D_2 are failure model parameters to be determined. E_{fmin} is the value of the plastic strain just before the failure.

3.3.3. Equation of State

This equation is used to relate the concrete density with the pressure, assuming that the concrete is compact without any gap. The formula is as follows:

$$P = K_1\overline{\mu} + K_2\overline{\mu}^2 + K_3\overline{\mu}^3 \quad (8)$$

where $\overline{\mu} = (\mu - \mu_{lock})/(1 + \mu_{lock})$ is the modified volumetric strain, where $\mu_{lock} = \frac{\rho_{grain}}{\rho_0} - 1$. ρ_{grain} is the density of the compact concrete without a gap, while ρ_0 is the initial density. μ_{lock} is the locking volumetric strain. K_1, K_2, K_3 are the model parameters to be determined.

All of the model parameters have been determined using a multi-variable regression based on the measured data from both quasi-static and Split Hopkinson Bar tests. At the end of the fitting process of Equations (5)–(8) for the unknown values of the model parameters to match the recorded experimental data, the values given in Table 4 were obtained. The parameters in Table 4 represent the material character of the ultra-high-strength concrete of 135 MPa strength investigated in this study.

Table 4. Parameters of JHC model for 135 MPa compressive strength concrete.

ρ (kg/m^3)	G,GPa	A	B	C	N	fc,MPa	T,MPa	EPS_O
2700	33.2	0.30	1.50	0.01	0.59	135	8.4	1.00
E_{fmin}	S_{fmax}	P_{crush},GPa	P_{lock},GPa	D1	D2	K1,GPa	K2,GPa	K3,GPa
0.001	12.5	0.162	0.000095	0.003	1.000	16.2	−40	26

The authors think that reliable material model parameters can be determined if the material characterization is performed considering data from all of the tests. This approach is based on the authors' unpublished previous experience with material characterization.

4. Discussion

Experimental works on the determination of concrete behavior using the Split Hopkinson Bar tests reported in the literature investigated the normal, high and ultra high-strength concretes, with or without fibers, employing generally greater sample sizes in terms of the height/diameter ratio [12–17,20–25]. In this study, smaller height/diameter ratios for samples have been preferred to achieve higher strain rates, as done in similar works [18,19]. It appears that numerical studies investigating the dynamic concrete behavior are not common in the literature.

A recent work in [24] presents the numerical results based on the JHC material model applied to a RPC with fibers. The present study has investigated an ultra high-strength concrete without fibers. The currently determined JHC model parameters differ from those obtained in [24], as expected due to the fiber effects. However, the order of magnitudes of the parameters are similar.

5. Conclusions

In this study, the design, production and the quasi-static testing of an ultra-high-strength (performance) concrete were carried out, leading to an average compression strength range of 125 to 135 MPa. These average values were measured for the samples tested on the 28th and 56th days following production. For the quasi-static compression tests, four sets of cylindrical samples with

the dimensions of Ø150 × 300 mm were used. In the SPHB tests, a total of 21 specimens with height/diameter ratios varying between 0.6 and 1.2 were used.

The concluding remarks that may be drawn from this study are given below:

- A new ultra-high-strength concrete mixture is designed, produced and tested under quasi-static and dynamic loading conditions.
- For quasi-static loading, the average compressive strength of the new mixture, depending on the testing day following production, varied between 108 and 135 MPa.
- For the dynamic testing conducted on a SHB test ring, it was observed that, for the same test conditions, as the height/diameter of a sample decreases, the measured strain rate increases.
- As expected, an increase in the test pressure increases the striker speed linearly. As a result of this, one can obtain the high strain rate deformation characteristics of the ultra high-strength concrete.
- High-strength concrete appeared to be sensitive to deformation rate. While the strain rate was 10^{-5} s^{-1} in quasi-static tests, the strain rate in the dynamic tests was measured in the range of 353–1288 s^{-1}.
- The maximum compressive stress values measured in the dynamic tests were observed to be 1.06–1.87 times higher than the quasi-static compression test average maximum compressive stress value of 135 MPa measured for specimens tested 56 days after production.
- Since the high-strength concrete has locally different constitutional characteristics (due to the aggregate, cement, GGBF slag, etc. distribution), it is considered that the strength performance at high strain rates may lay out in the range of 143–253 MPa.
- Generally, as the peak strain rate increases, the corresponding maximum compressive stress value appears to decrease.
- Time variations of stress, strain and strain rates recorded during the SPHB tests have been fitted to the JHC material model using an in-house developed computer code of multi-variable regression.
- The achieved strain rate values have been measured to be in the range that is generally observed in impact and blast conditions. Therefore, one may conclude that the model parameters determined are suitable for numerical simulations of this 135 MPa strength concrete.

In future work, ballistics tests on developed concrete samples are planned to determine the response of the UHSC under impact and blast loadings. In order to reduce the cost of such expensive tests, a numerical simulation program should be performed. This study is the first step towards achieving this objective.

Author Contributions: Methodology, A.R.G.; writing—original draft preparation, A.R.G.; validation, M.K.; writing—review and editing, S.K. and M.K.; supervision, S.K. All authors have read and agreed to the published version of the manuscript.

Funding: This research received no external funding.

Acknowledgments: This study was supported by YAPIRAY and TUBITAK SAGE. The authors acknowledge Ilhan Altinoz from YAPIRAY and Hakan Hafizoglu from TUBİTAK SAGE for their contributions to the studies on sintering.

Conflicts of Interest: The authors declare no conflict of interest.

References

1. Arioglu, E.; Kurt, G. Development of Very High Strength Concrete ın Yapi Merkezi: 1989 to 2007. In Proceedings of the 12th Concrete Prefabrication Symposium, Istanbul, Turkey, 13 November 2007.
2. Wu, C.; Li, J.; Su, Y. *Development of Ultra High Performance Concrete against Blast, From Material to Structures*; Woodhead Publishing: Cambridge, UK, 2018.
3. Kocataşkın, F. *Composition of the High-Strength Concrete*; Istanbul Technical University: Istanbul, Turkey, 1991.
4. Lavan, O.; de Stefano, M. Seismic behaviour and design of irregular and complex civil structures, Geotechnical. *Geol. Earthq. Eng.* **2013**, *24*. [CrossRef]

5. Puppio, M.L.; Giresini, L.; Doveri, F.; Sassu, M. Structural irregularity: The analysis of two reinforced concrete (r.c.) buildings. *Eng. Solid Mech.* **2019**, 13–34. [CrossRef]
6. Bischoff, P.H.; Perry, S.H. Compressive behaviour of concrete at high strain rates. *Mater. Struct.* **1991**, *24*, 425–450. [CrossRef]
7. Bresler, B.; Bertero, V.V. Influence of high strain rate and cyclic loading of unconfined and confined concrete in compression. In Proceedings of the Second Canadian Conference on Earthquake Engineering, Hamilton, ON, Canada, 5–6 June 1975; pp. 1–13.
8. Takeda, J.; Tachikawa, H. The mechanical properties of several kinds of concrete at compressive, tensile, and flexural tests in high rates of loading. *Trans. Archit. Inst. Jpn.* **1962**, *77*, 1–6. [CrossRef]
9. Hughes, B.P.; Gregory, R. Concrete subjected to high rates of loading in compression. *Mag. Concr. Res.* **1972**, *24*, 25–36. [CrossRef]
10. Watstein, D. Effect of straining rate on the compressive strength and elastic properties of concrete. *ACI J.* **1953**, *49*, 729–744.
11. Hughes, B.P.; Watson, A.J. Compressive strength and ultimate strain of concrete under impact loading. *Mag. Concr. Res.* **1978**, *30*, 189–199. [CrossRef]
12. Ngo, T.; Mendis, P.; Whittaker, A. A Rate Dependent Stress-Strain Relationship Model for Normal, High and Ultra-High Strength Concrete. *Int. J. Prot. Struct.* **2013**, *4*, 451–466. [CrossRef]
13. Yousuf, M.; Liew, R.; Tao, Z.; Shasha, W. *Dynamic Properties of Concrete Strength Using Split Hopkinson's Pressure Bar (SHPB) Test*; School of Engineering, University of Western Sydney (UWS): Sydney, Australia, 2011.
14. Guo, Y.; Gao, G.; Jing, L.; Shim, V. Response of high-strength concrete to dynamic compressive loading. *Int. J. Impact Eng.* **2017**, *108*, 114–135. [CrossRef]
15. Zhang, M.; Wu, H.; Li, Q.; Huang, F. Further investigation on the dynamic compressive strength enhancement of concrete-like materials based on split Hopkinson pressure bar tests. Part I: Experiments. *Int. J. Impact Eng.* **2009**, *36*, 1327–1334. [CrossRef]
16. Petrov, Y.; Selyutina, N. Scale and size effects in dynamic fracture of concretes and rocks. *EPJ Web Conf.* **2015**, *94*, 4005. [CrossRef]
17. Lu, Y.; Chen, X.; Teng, X.; Zhang, S. Dynamic compressive behavior of recycled aggregate concrete based on split Hopkinson pressure bar tests. *Lat. Am. J. Solids Struct.* **2014**, *11*, 131–141. [CrossRef]
18. Grote, D.; Park, S.; Zhou, M. Dynamic behavior of concrete at high strain rates and pressures: I. experimental characterization. *Int. J. Impact Eng.* **2001**, *25*, 869–886. [CrossRef]
19. Riisgaard, B.; Ngo, T.; Mendis, P.; Georgakis, C.T.; Stang, H. Dynamic increase factors for high performance concrete in compression using Split Hopkinson Pressure Bar. In Proceedings of the 6th International Conference on Fracture Mechanics of Concrete and Concrete Structures, Catania, Italy, 17–22 June 2007.
20. Hao, Y.F.; Zhang, X.H.; Hao, H. Numerical Analysıs of Concrete Material Properties at High Strain Rate Under Direct Tension. *Procedia Eng.* **2011**, *14*, 336–343. [CrossRef]
21. Hao, Y.; Hao, H. Mechanical properties and behaviour of concrete reinforced with spiral-shaped steel fibres under dynamic splitting tension. *Mag. Concr. Res.* **2016**, *68*, 1110–1121. [CrossRef]
22. Saadun, A.; Mutalib, A.A.; Hamid, R.; Mussa, M.H. *Behaviour of Polypropylene Fiber Reinforced Concrete under Dynamic Impact Load*; Department of Civil and Structural Engineering, Faculty of Engineering and Built Environment, Universiti Kebangsaan Malaysia: Bangi, Malaysia, 2016.
23. Lai, J.; Sun, W. Dynamic damage and stress-strain relations of ultra-high performance cementitious composites subjected to repeated impact. *Sci. China Ser. E Technol. Sci.* **2010**, *53*, 1520–1525. [CrossRef]
24. Lai, J.; Sun, W.; Xu, S.; Yang, C. Dynamic Properties of Reactive Powder Concrete Subjected to Repeated Impacts. *ACI Mater. J.* **2013**, *110*, 463–472.
25. Liu, J.; Sun, W.; Liu, J.; Shi, L. Dynamic mechanical behavior of ultra-high performance steel fiber reinforced concrete mixed with high volume fly ash under multi-impact compression. *J. Hebei Univ. Technol.* **2013**, *43*, 43–46.
26. Li, Q.; Meng, H. About the dynamic strength enhancement of concrete-like materials in a split Hopkinson pressure bar test. *Int. J. Solids Struct.* **2003**, *40*, 343–360. [CrossRef]
27. Forquin, P. Brittle materials at high-loading rates: An open area of research. *Philos. Trans. R. Soc. A Math. Phys. Eng. Sci.* **2017**, *375*, 20160436. [CrossRef]
28. Hao, Y.; Hao, H. Dynamic compressive behaviour of spiral steel fibre reinforced concrete in split Hopkinson pressure bar tests. *Constr. Build. Mater.* **2013**, *48*, 521–532. [CrossRef]

29. Cao, S.; Hou, X.; Rong, Q. Dynamic compressive properties of reactive powder concrete at high temperature: A review. *Cem. Concr. Compos.* **2020**, 103568. [CrossRef]
30. Hopkinson, B. A method of measuring the pressure in the deformation of high explosives or by the impact of bullets. *Philos. Trans. R. Soc.* **1914**, *A213*, 437–452.
31. Kolsky, H. An Investigation of the Mechanical Properties of Materials at Very High Rates of Strain. *Proc. Roy. Phys. Soc. B* **1949**, *62*, 676–700. [CrossRef]
32. Split-Hopkinson Pressure-Bar tests on Concrete and Mortar in Tension and Compression. *ACI Mater. J.* **1989**, *86*, 475–481.
33. Lee, O.S.; Kim, G.H. Thickness effects on mechanical behavior of a composite material(1001P) and polycarbonate in split Hopkinson pressure bar technique. *J. Mater. Sci. Lett.* **2000**, *19*, 1805–1808. [CrossRef]
34. Follansbee, P.S. *The Hopkinson Bar, in Metals Handbook*, 9th ed.; Mechanical Testing; American Society for Metals: Cleveland, OH, USA, 1985; Volume 8, pp. 198–203.
35. Holmquist, T.J.; Johnson, G.R.; Cook, W.H. A computational constitutive model for concrete subjected to large strains, high strain rates, and high pressures. In Proceedings of the 14th International Symposium on Ballistic, Quebec City, QC, Canada, 26–29 September 1993; American Defense Preparedness Association: Arlington, VA, USA, 1993; pp. 591–600.
36. Malvar, L.; Crawford, J.E.; Wesevich, J.W.; Simons, D. A plasticity concrete material model for DYNA3D. *Int. J. Impact Eng.* **1997**, *19*, 847–873. [CrossRef]